Soft modes in strained and unstrained rutile TiO_2

Pavlin D. Mitev,[1,2] Kersti Hermansson,[1,2] Barbara Montanari,[3] and Keith Refson[3]
[1]*Materials Chemistry, Ångström Laboratory, P.O. Box 538, SE-752 21 Uppsala, Sweden*
[2]*Theoretical Chemistry, Royal Institute of Technology, SE-100 44 Stockholm, Sweden*
[3]*STFC Rutherford Appleton Laboratory, Chilton, Didcot OX11 0QX, United Kingdom*
(Received 4 December 2009; revised manuscript received 6 February 2010; published 21 April 2010)

We have studied the lattice dynamics of crystalline TiO_2 using density-functional perturbation theory and the local-density approximation in a plane-wave pseudopotential formalism at equilibrium and uniaxially strained geometries. We present well-converged calculations of the dispersion curves, which sample a more complete volume of the Brillouin zone than in previous studies. We find an anomalously soft TA mode in a region of reciprocal-space previously unexplored either by any previous calculation or experiment. This is quite separate from the A_{2u} mode which becomes soft at the $\mathbf{\Gamma}$ point and is responsible for the incipient ferroelectric behavior. The harmonic frequency of the soft TA mode around $q=(\frac{1}{2},\frac{1}{2},\frac{1}{4})$ decreases to zero under an isotropic expansion with a strain slightly above 0.5% and we suggest that it may be possible to observe anomalous diffuse inelastic scattering corresponding to a dynamical instability using neutron scattering. In addition to the softening under isotropic strain, the frequency of this mode goes to zero under uniaxial strain along the [110] direction in *both* compression and expansion (at close to −0.5% and +1.0%, respectively), which offers new possibilities for experimental tests of softening under compressional strain. We further suggest that the soft TA mode may help explain the anomalously long-ranged convergence observed in previous calculations on slab models of the TiO_2 (110) surface by providing a mechanism for small changes in bonding at the surface to propagate deep into the bulk. The behavior of other modes under strain was also studied. The ferroelectric A_{2u} mode frequency is nearly independent of [110] strain, which contrasts with the behavior in response to [001] strain reported in the literature of a strong dependence. However, the frequency of the Raman-active B_{2g} mode does decrease to zero frequency under 1.3% strain, which should be observable using Raman spectroscopy.

DOI: 10.1103/PhysRevB.81.134303 PACS number(s): 63.20.D−, 71.15.Mb, 77.84.−s

I. INTRODUCTION

The extraordinarily complex range of behavior exhibited by TiO_2 has motivated a huge variety of experimental and theoretical studies by physicists, chemists, surface scientists, and materials scientists for many years. Pure stoichiometric TiO_2 has a rich phase diagram and there is still controversy regarding which of the rutile or anatase phases is the more stable under ambient conditions. It is an exemplar of transition-metal oxide behavior and the canonical system of surface science.[1] It is widely used in a diverse range of technological and industrial applications ranging from pigments, battery electrolytes, catalysis, solar cells, gas sensors, and optical coatings to name but a few. It is therefore no surprise that the properties of TiO_2 in the rutile crystal structure have been the subject of numerous experimental and theoretical investigations.

TiO_2 in the rutile crystal structure is an incipient ferroelectric, and has a large and strongly temperature-dependent dielectric constant. The consequent high refractive index of bulk and thin films is the basis of its utility in many technological applications, notably for optical antireflective coatings, dielectric mirrors, and pigments. A possible low-temperature ferroelectric phase transition was postulated on the basis of the low-temperature behavior of the experimental dielectric permittivity but has not been observed.[2] The microscopic origin of these dielectric properties has been investigated in a number of studies of the lattice dynamics using either force field approaches (Ref. 3, and references therein) or *ab initio* methods based on density-functional theory (DFT).[4–7]

The first lattice-dynamics study of rutile TiO_2 based on *ab initio* calculations is that by Lee *et al.*[4] In a comprehensive study based on density-functional perturbation theory (DFPT) (Ref. 8) they calculated phonon frequencies at the $\mathbf{\Gamma}$ point which are in agreement with infrared and Raman spectroscopic measurements, and Born effective charges and dielectric permittivity, also in good agreement with experimental values. The high dielectric constant was shown to be a consequence of a low-frequency (176 cm^{-1} in their calculations), "soft" A_{2u} mode and large Born effective charges (up to $7.3e-7.5e$ for Ti). Were the frequency of this mode to decrease to zero, it would correspond to the postulated ferroelectric phase transition, but it was found to have a positive frequency even in the athermal, 0 K limit.

Montanari and Harrison[5,6] focused on the behavior of the ferroelectric, transverse-optical (TO) A_{2u} mode. They demonstrated that this mode becomes soft at the $\mathbf{\Gamma}$ point if the lattice is expanded, either directly as a result of a negative effective pressure[5] applied to the local-density approximation (LDA)-optimized structure, or via the usual generalized gradient approximation (GGA) overestimate of the lattice parameter.[6] By applying a uniaxial expansive strain in the [001] direction, they predicted that the A_{2u} mode frequency should decrease to zero under a 3% expansive strain.

The *ab initio* studies mentioned above were confined to modes at the $\mathbf{\Gamma}$ point. The only *ab initio* investigation for other wave vectors that we are aware of is that of Sikora,[7] who used LDA calculations and a supercell-force-constant-matrix approach to compute phonon frequencies at several symmetry points of the Brillouin zone (BZ),[7] and the dispersion curves along a number of high symmetry directions in

the BZ. (The lattice dynamics of the other low-pressure polymorph of TiO_2, anatase, has also been investigated using density-functional perturbation theory.[9])

We present here an *ab initio* DFPT study of the lattice dynamics of rutile TiO_2 under the local-density approximation and using the plane-wave pseudopotential method. Our calculations include all long-ranged Coulomb interactions and nonanalytic terms responsible for LO-TO splitting, essential for a correct description of the dielectric properties. We have calculated accurate phonon dispersion curves which include regions of the Brillouin zone not sampled in any previous calculation. As a result, we have discovered a hitherto unsuspected, and large, volume of reciprocal space where the TA mode is extremely soft. We will investigate this mode in some detail and discuss possible experiments to detect the softening.

Inspired by the work of Montanari and Harrison[5] we also seek to identify potential soft-mode phase transitions as a function of strain. In this endeavor we have searched for completely soft modes within the entire Brillouin zone including the soft region around $(\frac{1}{2},\frac{1}{2},\frac{1}{4})$, and computed the response of the lattice dynamics to both isotropic and uniaxial applied strains (previous published work considered only uniaxial and [001] strains which preserve the tetragonal symmetry). In addition to uniform strain, we also consider [110] strains in both compression and expansion, which break the tetragonal space-group symmetry. The consequent splitting of the doubly degenerate soft TA mode allows the possibility of achieving a complete softening under compressive as well as expansive strain, a situation which could be more easily realized experimentally.

II. METHODS

The calculations used plane-wave pseudopotential implementation of DFPT as implemented in the CASTEP code.[10,11] With one exception the calculations were performed using the LDA (CA-PZ) (Ref. 12) functional. Montanari and Harrison showed that the LDA gives a better description than GGA of the ferroelectric mode, which has an imaginary frequency at the equilibrium GGA lattice parameters.[6]

Pseudopotentials were created using the "optimized" method of Rappe *et al.*[13] The Ti pseudopotential was constructed to leave the semicore $3s$ and $3p$ states as valence as in Refs. 4 and 14 with core radii $r\_c=1.32(3s)$ $1.45(3p)$ $1.53(3d)$ tuned to also give an accurate $4s$ pseudo wavefunction. The d projector was used as the local component. The oxygen pseudopotential was an optimized potential using the method of Lin *et al.*[15] with $r\_c=1.4$ a.u. and a separate mixed local component. Both pseudopotentials are fairly hard and a plane-wave cutoff of 1100 eV was used yielding a maximum error in forces of <1 meV/Å and stress of <0.011 GPa. The electronic sampling of the BZ was performed using a $4\times4\times6$ grid of k points using the Monkhorst-Pack scheme,[16] at which level forces are converged to better than 0.4 meV/Å and stresses to 0.01 GPa. Comparison of structural parameters with other accurate calculations (Table I) shows this combination to be of high accuracy.

Equilibrium lattice parameters were determined using the Broyden-Fletcher-Goldfarb-Shanno (BFGS) algorithm which optimized both the cell parameters and internal coordinates simultaneously. A finite-basis set correction[24] was used to compensate for the error caused by Pulay stresses.

Phonon-dispersion curves were calculated using density-functional perturbation theory in conjunction with the method of Fourier interpolation of dynamical matrices.[8,25] The cumulant sum method of Parlinski[26] was used to construct the aperiodic force constant matrix in real space. In this case of rutile TiO_2 a $5\times5\times7$ grid of q vectors gave interpolation error over the entire BZ of less than 13 cm^{-1} with a mean error per q point <3 cm^{-1}. When plotting the dispersion curves we used a very fine sampling of the q-space path combined with an algorithm which uses eigenvector matching to correctly determine crossing or avoidance behavior where branches meet. This gives a high degree of confidence in the connectivity of our dispersion curves. The nonanalytic contribution to the dynamical matrix which describes LO-TO splitting at the $\mathbf{\Gamma}$ point was calculated from Born effective charges and dielectric permittivities obtained using DFPT response to an electric field.[25]

III. RESULTS

A. LDA equilibrium structure and Γ-point phonons

The optimized cell parameters are listed in Table I together with previous literature results. Our calculated lattice parameters are slightly smaller (0.01–0.02 Å) than those from a low-temperature neutron-diffraction experiment,[19] as expected from the LDA. The magnitude of the error due to the pseudopotential approximation may be obtained from a comparison with projector augmented wave (PAW) and with all-electron (AE) full-potential linearized augmented-plane-wave (FP-LAPW) calculations[20,21] and there is agreement in the lattice parameters to around 0.5%. Born effective charges are in agreement with previous pseudopotential calculations at the level of 3% or better but dielectric permittivities differ by around 5%.

There are small but significant discrepancies with equilibrium lattice parameters obtained in some of the earlier pseudopotential calculations,[4] which were lower than the all-electron LDA values by approximately the same degree as the overestimation in our calculation. The origin of this discrepancy is probably associated with the different methods of pseudopotential generation used [optimized Rappe-Rabe-Kaxiras-Joannopoulos (RRKJ) in our case and Troullier-Martins in the earlier calculation]. Adjusting the core radii of the pseudopotential and employing a "designed nonlocal"[27] projector scheme made very little difference to the optimized structure. Using the FP-LAPW values 4.558 Å and 2.920 Å as estimates for the converged a and c parameters at the all-electron LDA level, we note that our parameters are about 0.3% and 0.8% too large, respectively. We have therefore also calculated the phonon frequencies for a uniformly contracted structure (by 0.5%), and Tables II and III list the computed frequencies at the $\mathbf{\Gamma}$ point and at several high-symmetry points on the Brillouin-zone boundary, respectively.

TABLE I. Calculated and reference structural parameters, Born effective charges (principal values) Z^* (e) and dielectric permittivity ε_c^∞ of TiO_2 rutile.

	a (Å)	c (Å)	u	c/a	Ω (Å^3)
This work	4.572	2.943	0.304	0.644	61.520
X ray 100 K[a]	4.582	2.953	0.305	0.644	61.997
X ray 298 K[b]	4.594	2.959	0.305	0.644	62.432
Neutron 15 K[c]	4.587	2.954	0.305	0.640	62.154
AE-FLAPW-LDA[d]	4.558	2.920	0.304	0.641	60.664
LCAO-LDA[e]	4.555	2.929	0.304	0.643	60.771
PW-LDA (PAW)[e]	4.557	2.928	0.304	0.643	60.804
PW-LDA[f]	4.536	2.915	0.304	0.643	59.980
PW-LDA[g]	4.545	2.919	0.304	0.642	60.298
PW-LDA[h]	4.567	2.933	0.304	0.642	61.189

	Ti			ε	
	$Z^*_{[110]}$	$Z^*_{[1\bar{1}0]}$	$Z^*_{[001]}$	$\varepsilon^\infty_{a,b}$	ε^∞_c
This work	7.492	5.425	7.768	7.950	9.212
FLAPW[d]	7.19	5.20	7.70		
LDA[e]	7.372	5.322	7.752		
LDA[f]	7.335	5.343	7.541	7.535	8.665
Expt.[i]				6.843	8.427

[a]Reference 17.
[b]Reference 18.
[c]Reference 19.
[d]Reference 20.
[e]Reference 21.
[f]References 4 and 22.
[g]Reference 6.
[h]Reference 7.
[i]Reference 23.

The Γ-point frequencies listed in Table II exhibit unsatisfactorily large discrepancies between different calculations given that all aim to reproduce the limiting value within the LDA. Nevertheless some trends can be observed and conclusions drawn. The physical approximation which differs among these and our calculations is the pseudopotential approximation and the detailed recipe used for construction of the pseudopotentials. (It is unlikely that inadequate convergence is responsible for the variation. Our computed frequencies are converged with respect to both plane-wave cutoff and Brillouin-zone sampling to 2 cm^{-1} or better for most modes and at worst 5 cm^{-1}. Most of the previous calculations appear similarly well converged.) The origin of much of the variation can be attributed to the secondary effect of the different equilibrium lattice and internal parameters resulting from the different pseudopotentials. Table II demonstrates the effect of performing a calculation under a uniform compressive strain of −0.5%, which brings the frequencies into much closer agreement with the all-electron FP-LAPW results. The largest errors remain in the B_{1g}, E_u, and A_{2u} modes which all have very large pressure dependencies and mode Gruneisen parameters.[5] These results suggests that the best approximation to all-electron LDA values from our pseudopotentials is obtained at −0.5% strain.

B. Phonon-dispersion relations

Phonon-dispersion curves obtained using Fourier interpolation of dynamical matrices along selected high-symmetry directions in the Brillouin zone are plotted in Fig. 1. It is evident that the experimental frequencies are reproduced to an accuracy of 20 cm^{-1} or better by our LDA pseudopotential calculation with the exception of the Γ-**Z** transverse-acoustic branch where the discrepancy rises to nearly 40 cm^{-1}.

An unexpected feature apparent in the dispersion curves shown in Fig. 1, is that the lowest-frequency mode is the transverse-acoustic mode at the Brillouin-zone boundary along the **M**-**A** direction, at roughly $q=(\frac{1}{2},\frac{1}{2},\frac{1}{4})$ with a frequency of 42 cm^{-1}. This feature of the lattice dynamics has not been previously reported, as no published calculation or experiment has explored this region of the Brillouin zone. A similar feature has been reported in some unpublished calculations.[31] It will be shown that this mode may have important consequences for the relative structural stability of the rutile and anatase phases, for the behavior of surfaces and may be detectable in experiment. It is therefore important to establish that this phenomenon is a correct prediction of density-functional theory within the LDA, and is not an artifact of pseudopotential error or interpolation error (convergence error has already been ruled out). To this end we have performed additional DFPT calculations of the phonon-dispersion curves using an alternative norm-conserving pseudopotential for Ti. This was constructed with larger core radii and used the "designed nonlocal" method to ensure accuracy of the 4s wave functions.[27] The resulting dispersion

TABLE II. Calculated and experimental phonon frequencies ω (cm^{-1}) of TiO_2 rutile at the Γ point. The corresponding deviations from the FPLAPW results are given in parentheses. Experimental frequencies in square brackets denote low-temperature measurements.

Mode	PBE[a]	PW91[a]	LDA[a]	LDA[b]	FLAPW[c]	LDA[d]	Neutron[e]	IR& Raman[f,g]	This work 0%	This work −0.5%
						Raman				
B_{2g}	775	781	825(+9)	828(+12)	816	801(−15)	825	827	805(−11)	823(+7)
A_{1g}	566	572	612(0)	623(+11)	612	616(+4)	610	612 [611]	601(−11)	617(+5)
$E_g(2)$	429	434	463(−1)	472(+8)	464	472(+9)	445	447 [455]	457(−7)	469(+6)
B_{1g}	154	152	137(−1)	125(−13)	138	132(−6)	142	143 [143]	130(−8)	115(−23)
						Silent				
A_{2g}	424	425	422(+6)	416(−1)	416	413(−3)	Not found		405(−11)	407(−9)
B_{1u}	358	363	393(−5)	408(+9)	398	418(+19)	406		385(−13)	401(+2)
B_{1u}	79	99	104(−8)	117(+5)	112	118(+6)	113		101(−11)	112(+1)
						Infrared				
E_u(TO)	469	472	488(+1)	493(+6)	487	499(+12)	494	500	476(−12)	485(−2)
E_u(TO)	354	357	384(−1)	391(+7)	385	393(+9)	Not found	388	375(−10)	388(+4)
E_u(TO)	124	127	191(+35)	165(+8)	156	144(−13)	189	183	127(−29)	146(−10)
A_{2u}(TO)	*i*86	47	154(+1)	176(+23)	153	192(+39)	173 [142]	167 [144]	126(−27)	164(+11)
A_{2u}(LO)				769(−15)	784	801(+17)	811		749(−35)	761(−23)
E_u(LO)				808(+1)	808	788(−20)	807	842	782(−26)	803(−5)
E_u(LO)				442(+1)	441	435(−6)	458	429	432(−9)	439(−2)
E_u(LO)				352(−4)	355	353(−2)	373	375	342(−13)	341(−14)

[a]Reference 6.
[b]Reference 4.
[c]Reference 20.
[d]Reference 7.
[e]Reference 28.
[f]Reference 29.
[g]Reference 30.

curve (see supplementary material[32]) does not differ significantly and the anomalous soft mode is still present. We also performed finite-difference phonon calculations in a supercell using very accurate Vanderbilt ultrasoft pseudopotentials. These yielded structural parameters of $a=4.553$, $c=2.921$, $u=0.304$ which are within 0.1% of the all-electron LAPW values of Table I. The acoustic-phonon frequencies at **M**, $(\frac{1}{2},\frac{1}{2},\frac{1}{4})$ and **A** are 59 cm^{-1}, 31 cm^{-1}, and 91 cm^{-1}, respectively, compared to 71, 47, and 83 cm^{-1} for the our DFPT calculation using norm-conserving pseudopotentials. (For full set of computed frequencies see supplementary material.[32]) The midsegment softening is therefore robustly reproduced and if anything our DFPT calculations underestimate its magnitude.

Our dispersion curves show a flattening toward **Γ** of the high-frequency modes along **Γ**-**Z** and **Γ**-**M**, and the shape is in good agreement with the inelastic neutron-scattering (INS) measurements except for a small rigid downshift in frequency. There is no sign of the overbending reported by Sikora[7] along these directions or along the LA mode toward the **M** point. Our result shows that this mode does not cross the flat B_{1u} mode but becomes degenerate with it only at the **M** point itself. Along direction **Γ**-**X** we see an almost dispersionless topmost B_{2g} mode at 805 cm^{-1}, which becomes degenerate with the LO E_u mode at the **M** point. These two branches are downshifted with respect to experimental measurements, as already noted at the **Γ** point, but the shape is in reasonable agreement. Again there is disagreement with the result of Sikora (Fig. 1 in that paper), which shows a dispersion of around 50 cm^{-1} in both modes, and a strong overbending in the topmost mode. Along **Γ**-**Z**, the dip in the curve at around $(0,0,\frac{1}{3})$ observed in the experiment is well reproduced in our calculations, although the overall frequency is uniformly lower than experimentally observed.

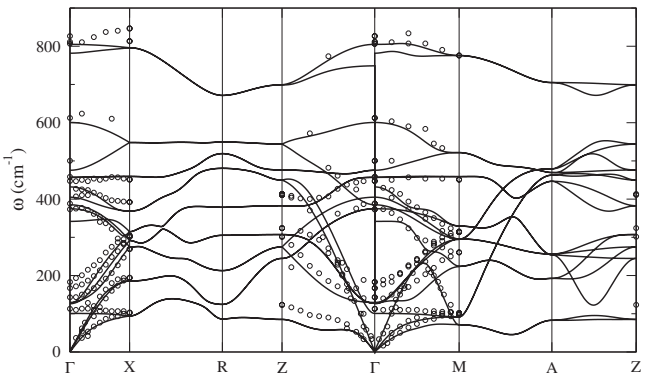

FIG. 1. Calculated phonon dispersion of TiO_2 rutile compared with inelastic neutron-scattering experiment (Ref. 28).

TABLE III. Calculated in this work, reference LDA calculation (Ref. 7) and experimental (Ref. 28) phonon frequencies ω (cm^{-1}) of TiO_2 rutile at the high-symmetry points **X**, **M**, **Z**, **A**, and **R** of Brillouin zone.

X			**M**			**Z**			**A**		**R**	
This work	LDA	Expt.	This work	LDA	Expt.	This work	LDA	Expt.	This work	LDA	This work	LDA
						Optical modes						
92	109	103	76	106	102	245	248		192	223	85	136
275	281	269	227	241	261	275	281	302	253	259	213	223
287	318	301	295	304	314	307	318	324	256	261	305	310
315	324	305	297	332	315	384	431	411	446	470	378	422
369	381	392	333	360		449	452	414	463	483	480	498
461	481	451	459	475	452	477	514		469	486	518	523
548	572		523	542		545	567		478	504	548	588
800	806	847	775	760	776	698	709		705	721	673	681
						Acoustic modes						
89	109	103	77	73	98	84	104	123	80	97	84	105
184	193	194	87	106	102	447	431	414	463	(465)[a]	126	136

[a]The number in brackets is taken from the graph instead from the table published in Sikora's paper Ref. 7, Table 3.

An explanation of the general observation that many modes in our calculation display much smaller dispersion than in the calculation of Sikora (not only the topmost modes and the **Γ**-**M** TA mode but throughout the frequency spectrum and BZ) can be found in consideration of the behavior of long-ranged tails of the interatomic force constants. Sikora's calculation used a supercell which faithfully represents force constants out to a distance of some 4.5 Å in the plane and 3 Å in the *c* direction without aliasing errors. By contrast, our calculation using an interpolation from a grid, considers force constants out to over 11 Å in all directions, and is almost fully converged. Ackland *et al.*[33] showed that in the case of the phonon dispersion of silicon, it is necessary to include force constants out to sixth neighbors to correctly reproduce the flat approach of the TA branch to the **X** point, and that truncating the force constant matrix at a smaller

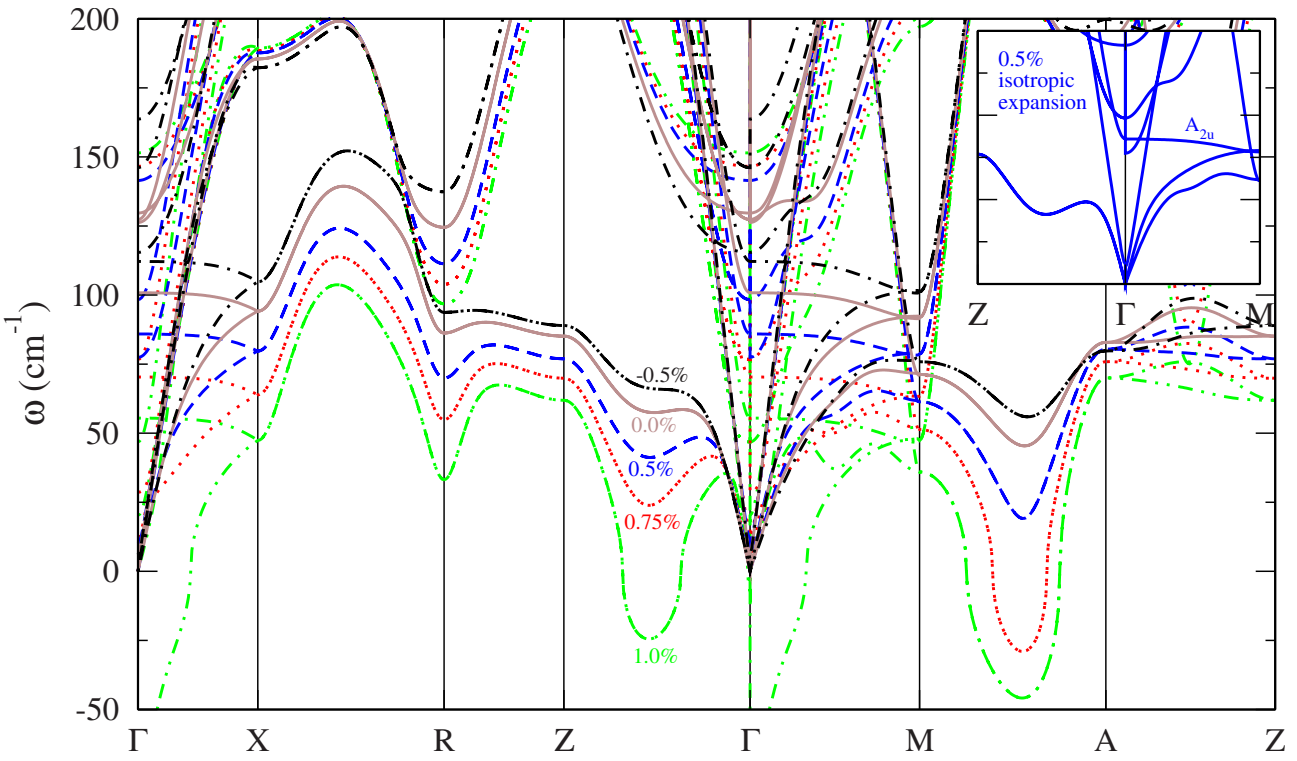

FIG. 2. (Color online) Calculated phonon dispersion of TiO_2 rutile under uniform isotropic expansion. Inset shows behavior of A_{2u} mode at 0.5% expansion.

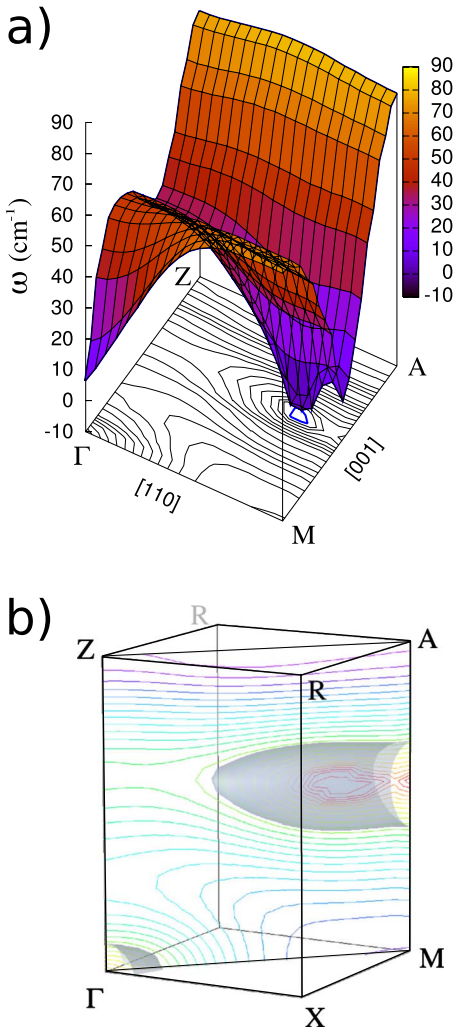

FIG. 3. (Color online) (a) Variation in TA mode frequency across Brillouin zone showing minimum at low-symmetry point slightly offset from **M**-**A** midpoint. (b) Three-dimensional locus of lowest-frequency region of TA mode showing a cigar-shaped region of low frequency.

radius has the effect of erroneously predicting too large a dispersion. The long-ranged nature of the force constant matrix was attributed to the strong covalent bonding network in silicon. Clearly a similar effect operates in rutile TiO_2 which suggests that a substantial degree of covalency is present. It appears that the dispersion curves plotted by Sikora suffer from aliasing error and can only be considered accurate for wave vectors at the Brillouin-zone center and boundaries.

C. Behavior of the soft acoustic mode

1. Uniform expansion of the lattice

Given that the incipient ferroelectric behavior of rutile TiO_2 has been of considerable interest, and the prediction of Montanari and Harrison of a hypothetical phase transition upon application of an expansive strain there is clearly a strong motive to investigate whether the softening near $q=(\frac{1}{2},\frac{1}{2},\frac{1}{4})$ could lead to any new phenomena. We have therefore studied the effect on the frequencies of applying an isotropic strain to the unit cell. Expansions of 0.5%, 0.75%, and 1.0% of the a and c lattice parameters were considered and the internal coordinate, u, was optimized at each strain. The region of the spectrum below 200 cm^{-1} is shown in Fig. 2. More complete dispersion curves are deposited as additional material. As established in previous work, the A_{2u} mode at **Γ** has a large mode Gruneisen parameter of 13.5 and becomes soft at 0.75% expansion. However the onset of mechanical instability is not governed by this mode but rather by the acoustic mode in the region of $(\frac{1}{2},\frac{1}{2},\frac{1}{4})$ which becomes soft at a strain of 0.5%. The second dip observed in the LA mode halfway along the **Γ**-**Z** branch also drops to zero frequency at 0.75% strain.

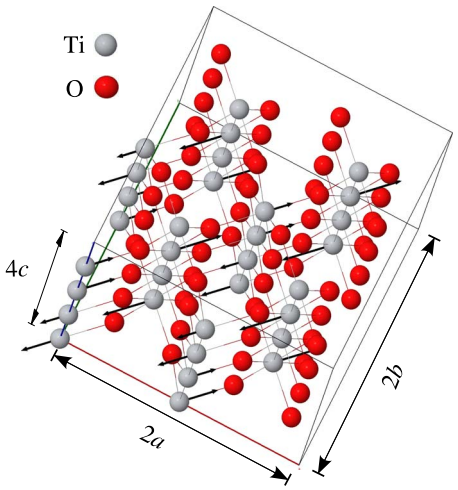

FIG. 4. (Color online) Eigenvectors of soft mode at $(\frac{1}{2},\frac{1}{2},\frac{1}{4})$ point shown in $2\times2\times4$ supercell.

The existence of soft modes under expansion at two points of low symmetry raises the question of the behavior at other wave vectors not plotted in Fig. 1 and 2. To investigate this we computed the frequencies on a grid of wave vectors in order to map the extent and shape of the soft region of reciprocal space. (The Fourier interpolation lattice-dynamical method is not restricted to the high-symmetry directions and allows the mapping of modes across the entire Brillouin zone at insignificant additional computational cost.) Figure 3(a) shows a contour and three-dimensional plot of frequencies for a 0.5% expansion projected along the plane. A "valley" of low frequencies extends along the direction joining the "dip" halfway along **M**-**A** to that halfway along **Γ**-**Z**. It can be seen that the lowest frequency does not lie on any point of symmetry but close to (0.3625,0.3625,0.2768). An alternative representation of the soft region is shown in Fig. 3(b), where it can be seen that the lowest frequencies are found in a cigar-shaped region with its long axis along [0,0,1]. At 0.75% expansion this region has elongated to a cylinder which touches the c^* axis along **Γ**-**Z**, where the acoustic mode becomes soft at roughly $(0,0,\frac{1}{3})$. The ferroelectric A_{2u} mode only reaches zero at 0.75% expansion.

Thus the first onset of a soft mode in TiO_2 upon expansive strain does *not* occur for the ferroelectric A_{2u} mode at the **Γ** point but on a cylinder of reciprocal space centered around (0.3625,0.3625,0.2768) and lying along [001]. Given that the

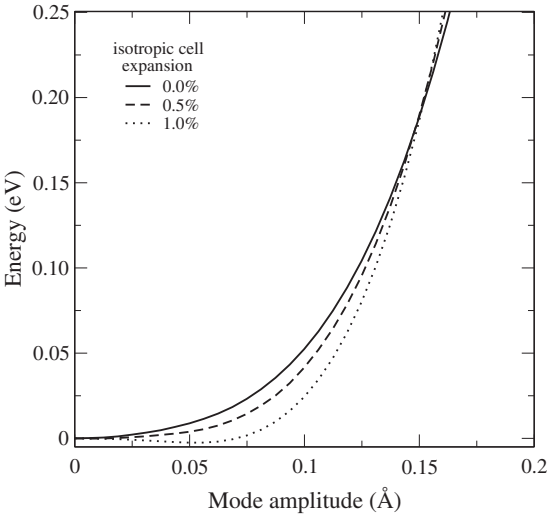

FIG. 5. Potential-energy surface as a function of amplitude of frozen soft TA mode at $q=(\frac{1}{2},\frac{1}{2},\frac{1}{4})$. *X* axis label is Ti ion displacement in angstrom.

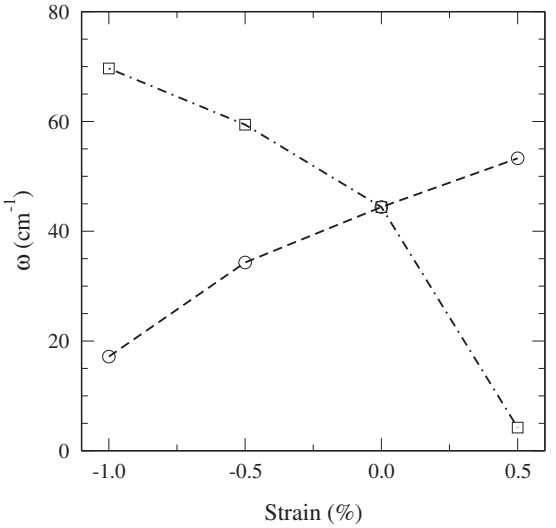

FIG. 6. Effect of anisotropic [110] strain on phonon-dispersion curves. The symmetry-breaking strain lifts the degeneracy of the TA modes along the **M**-**A** direction.

0.5% compressive strain frequencies are in best agreement with experiment, it is most likely that the onset of any elastic instability would occur at an expansive strain between 0.75% and 1%.

The eigenvectors of the soft mode at $q=(\frac{1}{2},\frac{1}{2},\frac{1}{4})$ are plotted in a $2\times2\times4$ supercell in Fig. 4, which shows that the atomic displacements of all atoms are directed parallel to the [110] direction and consist mainly of a displacement of the Ti atoms relative to the oxygen octahedra, which are only slightly distorted. Alternate planes are moving in antiphase and the motion within each plane consists of an in-plane antiphase shearing of pairs of layers. An animation of this mode is included in the supplementary material[32] as well as full dispersion plots for the strained calculations described above.

2. Mode potential-energy surface

All the frequencies above are computed using the harmonic approximation, which however breaks down in the vicinity of a phase transition. To investigate further what predictions can be made of the physical behavior consequent to this softening we investigated in detail the shape of the potential-energy curves involved. Frozen phonon calculations were used to map the potential-energy surface for the soft acoustic mode at a wave vector of $q=(\frac{1}{2},\frac{1}{2},\frac{1}{4})$ and the result is plotted in Fig. 5. As might be expected a double-well potential appears with a minimum located at a maximum Ti displacement of 0.065 Å and a depth of only 2.5 meV.

This is clearly a substantially anharmonic mode potential-energy surface and the assumptions of harmonic lattice-dynamics theory break down for this mode. A proper anharmonic treatment of the quantum-mechanical nuclear motion would yield the nuclear wave function and excitation energies of the transitions, corresponding to frequencies which could be experimentally observed. A full quantum-mechanical calculation would involve computing the multi-dimensional potential-energy surface and solving the Schrödinger equation for all of the relevant degrees of freedom. (At least two for this degenerate mode.) Such a calculation is beyond the scope of this work but a few conclusions on the character of the solution which arise from general principles may be relevant. Anharmonic quantum oscillator models in potentials with shallow double wells tend to yield singly peaked and centered solutions, and no symmetry breaking is predicted. In this case the well depth of 2.5 meV is much smaller than the thermal energy predicted by the equipartition theorem for an individual mode of roughly 25 meV at 300 K. This would tend to suggest that no phase transition will be observed even substantially below room temperature. However these conclusions, based on a one-dimensional oscillator model, will be modified by the degenerate pair of modes and coupling to the other lattice modes. This must, in principle, alter the potential-energy surface and may give rise to unexpected behavior.

3. Uniaxial strain

The possibility that some interesting consequences for materials properties might result from the softening of the acoustic branch away from the **Γ** point motivated us to consider what mechanisms might drive this mode to zero frequency. There are clear obstacles to any experimental measurement of the softening under uniform dilation. This can be achieved by thermal expansion but high temperatures would make inelastic experiments difficult. And any latent soft-mode phase transition to a lower symmetry phase would be thwarted by thermal motion. Alternatively, doping with a larger cation or anion could also cause expansion but in this case the mass defect effect is likely to be large and not separable from the volume effect. However, uniaxial strains may be generated experimentally by thin-film deposition on a substrate which may be "bent" to apply either a compressive or expansive strain.[34] Montanari and Harrison showed that the A_{2u} mode frequency has a strong dependence *uniaxial*

strain along the [001] axis, decreasing to zero at +3% strain. However, the [110] direction is probably more relevant to many experiments as it is perpendicular to the most common cleavage plane and most stable surface plane. A strain along the in-plane [110] axis breaks the C_4 symmetry axis and unlike the [001] strain splits the degenerate mode. Such splitting must decrease the frequency of one or other of the formerly degenerate modes under infinitesimal strain, which motivates a study of their behavior under finite strain.

We performed simulations under applied uniaxial strains along [110] of −1%, −0.5%, and 0.5%. The internal coordinates were fully relaxed and the lattice dynamics was recomputed. The results are plotted in Fig. 6. As anticipated, the degenerate mode is split in the strained calculations. One of the split modes decreases to zero frequency under uniaxial expansion as it does under uniform expansion. But in addition, the other of the pair also becomes soft under compressive strain. This raises new experimental possibilities for a physical realization of the soft mode. A 1% compression would occur at 2.7 GPa, well within the range achievable by, for example, a Paris-Edinburgh cell as used in inelastic neutron scattering. While high-pressure INS experiments under controlled anisotropic strain are not common, it is possible that such an experiment could be feasible.

According to the most recent experimental evidence (Ref. 35, and references therein), uniaxial expansion perpendicular to [110] also occurs experimentally as a consequence of outward relaxation at the (110) surface, which otherwise retains very similar to the cleaved bulk.[36] Bredow *et al.*[37] predicted an outward relaxation of the second (110) surface layer of around 0.5% using *ab initio* DFT methods, and there is experimental evidence of expansion in TiO_2 nanocrystals.[38] It is plausible that our predicted bulk soft mode might have an analogous mode at the TiO_2 (110) surface and that relaxation of surface layers could precipitate softening behavior. Soft behavior has actually been observed as a function of temperature in (110) TiO_2 using time-of-flight He atom surface scattering.[36] That study probed only surface modes and the relationship to the bulk phonons in the present study would only be possible to establish by much more expensive direct *ab initio* calculations of lattice dynamics of the surface which are beyond the scope of the present work. It is not possible to conclude that any of the theoretical predictions of soft modes have been experimentally confirmed. However, the experimental evidence does point to behavior which is plausibly related but which would need further theoretical work to establish a truly comparable prediction.

D. Behavior of the ferroelectric A_{2u} mode

The softening behavior of the A_{2u} ferroelectric mode under expansive strain or negative pressure has previously been discussed in considerable detail.[5] Nevertheless an examination of the q dependence of this mode allows us to expand on this previous work and reveals a hitherto unsuspected richness of behavior.

The ferroelectric A_{2u} mode has a large Gruneisen parameter, and its frequency drops from 126 cm^{-1} at 0% expansion to 76.9 cm^{-1} at 0.5% uniaxial expansion, where it dips below the B_{1u} mode. However, it can be seen in the inset of Fig. 2. that despite its larger dispersion, it does not cross the B_{1u} mode but instead these two modes mix and have an avoided crossing very close to **Γ** at (0.04,0.04,0). The B_{1u} mode becomes connected to a mode rising to nearly 300 cm^{-1} at **M** and A_{2u} connects to the higher of the two *acoustic* branches at **M**. At a larger expansion of 0.75%, the A_{2u} mode drops to less than 9 cm^{-1}, which is the onset of softening within the accuracy of this calculation. At this expansion the two transverse-acoustic branches have become almost degenerate all the way from **Γ** to **M**. This degeneracy allows yet another exchange of mode character along the **Γ**-**M** line as the expansion is increased to 1.0%, where the A_{2u} mode has mixed with one of the TA modes where they became degenerate at the **M** point and again switched connectivity between the one TA mode and the other. At this, the highest positive strain we considered, the very highly kinked avoided crossing is still present but is now between a TA mode and the B_{1u} mode at 50 cm^{-1}. The A_{2u} mode now rises smoothly to join the TA modes at **M**.

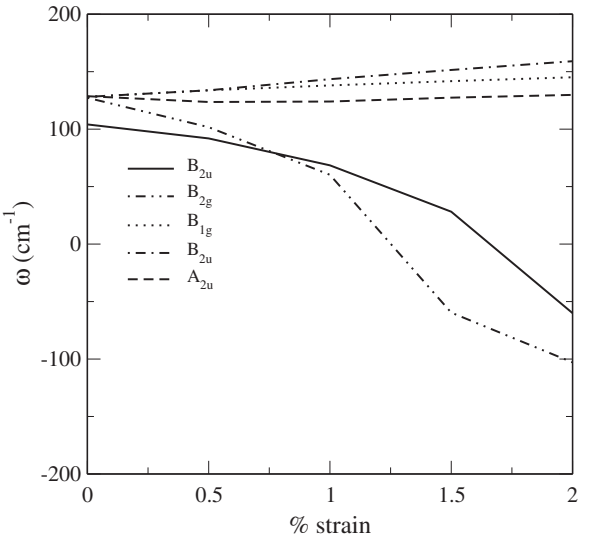

FIG. 7. Frequencies of five lowest-frequency modes at the **Γ** point under anisotropic strain. The ferroelectric A_{2u} mode is not sensitive to strain in this direction but the B_{2u} and B_{2g} modes become soft.

We also calculated the response of the A_{2u} and other modes at the **Γ** point to a uniaxial strain along [110]. The result is reported in Fig. 7. In contrast to the behavior reported by Montanari and Harrison[5] where the A_{2u} mode frequency showed a strong dependence on the amplitude of a [001] strain, indeed approaching zero at 3% strain, we find very little sensitivity to a [110] strain. It can be seen, however, that the inactive B_{2u} mode and the Raman-active B_{2g} mode do exhibit a strong response to strain in this direction, becoming soft at 1.6% and 1.3% expansive strain, respectively.

IV. DISCUSSION

A. Consequences of the bulk soft mode

We now consider the observable consequences the predicted bulk soft mode near $q=(\frac{1}{2},\frac{1}{2},\frac{1}{4})$. Our calculations do

not predict a soft-mode phase transition under easily realized experimental conditions. Although a lattice expansion of 0.5% can be induced by heating to around 600 °C the thermal energy per mode of roughly 75 meV is considerably larger than the well depth of 2.5 meV which is sufficient to ensure that no symmetry breaking by the double well will occur. Indeed it is probable that zero-point energy would be sufficient to symmetrize the wave function of the quantum oscillator of the mode at low temperatures even if a low-temperature expansion of the lattice could be achieved. However, it might be possible to measure the anharmonicity of the mode using high-resolution inelastic neutron- or x-ray scattering techniques at elevated temperatures. (Anomalous diffuse scattering due to phase transition precursor dynamical effects has been measured in insulating crystals, for example, in the inelastic neutron-scattering measurements on $CaCO_3$ of Harris *et al.*[39] found anomalous scattering with a strong temperature dependence, which was shown to be related to a high-pressure phase transition due to a soft mode at the **F** point).

The thermodynamic stability of the rutile phase of TiO_2 with respect to the anatase polymorph has been the subject of several studies in the literature (Ref. 21, and references therein). Despite a 10% difference in density the difference between the ground-state energies of the two phases is extremely small—less than 0.05 eV for an LDA/PAW calculation[21]—rather less than the variation among different exchange correlation functionals within DFT and other Hamiltonians. However, a rigorous prediction of relative stability must be based on the thermodynamic free energy and include the effect of vibrational entropy. We wish to emphasize that this contribution can be significant compared to the electronic total-energy difference. The contribution due to the soft acoustic phonon at 80 cm^{-1} in our calculations contributes also approximately 0.05 eV at 300 K and the additional lowering due to the anomalous soft cigar-shaped region can be estimated at roughly 0.025 eV, again comparable to the computed total-energy difference.

B. Long-ranged surface relaxation in (110) thin films

A phenomenon which has been much discussed in the literature relating to simulation of TiO_2 surface properties concerns anomalous convergence behavior of thin film or "slab" models containing a pair of (100) surfaces. Substantial oscillations with thickness are seen in surface energies, atomic displacements, electronic band edges, and work function, depending on whether there is an odd or even number of trilayers in the slab. These oscillations decay slowly with distance; convergence is only achieved with slabs of more than ten layers or 32 Å thickness.[3,37,40–48] This phenomenon has hindered theoretical work on the TiO_2 surface by making accurately converged calculations computationally expensive. The resulting lack of agreement on the precise quantitative *ab initio* prediction of surface relaxation in TiO_2 (110) is particularly unfortunate in view of the controversy in the experimentally measured surface structure using different techniques which has only recently been resolved (see Refs. 35 and 49). All of the aforementioned works contain quantitative analyses of the oscillatory and long-ranged convergence behavior but the only attempt at an explanation is put forward by Bredow *et al.*[37] That article analyzed the electronic structure of even- and odd-layered slab models and discovered a larger peak in the electronic density of states (DOS) of the even-layered slab corresponding to an enhanced hybridization between Ti $3d$ and O $2p$ states which results in stronger bonding between the first and second layers. Though no spatial resolution of the DOS was presented, this enhanced bonding presumably arises from the under coordination of the surface oxygen atoms. Bredow *et al.* then make the argument that the important distinction between odd- and even-layered systems is the presence or absence of a central plane of symmetry. However, this does not stand as a complete explanation of the origin of the specific anomalous behavior of TiO_2 (110). A satisfactory explanation ought to include a reason why TiO_2 (110) is unusual in this regard. All oxide surfaces have undercoordinated oxygen which can lead to enhanced bonding with lower layers. Furthermore, with the exception of the surface layer atoms, where the coordination is deficient, it is not clear whether changes in electron density and DOS with depth are a primary cause of, or a consequence of, geometric relaxation.

What is needed to complete the explanation is an account of why a perturbation of the cleaved geometry at the surface has an effect deep inside the bulk specifically in TiO_2. In other words, is there a structural instability in the bulk; a high compliance which would allow long-ranged propagation of a displacement arising at the surface deep into the bulk? We suggest that the bulk soft mode around $q=(\frac{1}{2},\frac{1}{2},\frac{1}{4})$ provides just such a mechanism. The eigenvectors of the soft mode for a 0.5% [110] uniaxial expansion lie along the [110] direction for Ti ions, normal to the (110) surface, with smaller antiphase displacements in almost the same direction of the O ions. These are very similar to the eigendisplacements of the unstrained system shown in Fig. 4 and in the supplementary material.[32] Consequently, a layer displacement perpendicular to the (110) surface of a slab, with alternating odd/even sign, has a very large projection onto the soft bulk eigenvector. Below the second layer, the latest experiments[35,49] and converged slab calculations agree that the structure is very similar to bulk TiO_2. Therefore bulk crystal modes should give a reasonably good approximation to the subsurface dynamics. The small, oscillatory layer relaxations are similar to those of the strained bulk calculation, which resulted in a decrease in one acoustic mode to a frequency close to zero.

We therefore propose the following explanation of the anomalously slow and oscillatory convergence behavior with slab thickness. Similar to Bredow *et al.*'s analysis the undercoordination of the surface oxygen lone-pair orbitals results in strengthened Ti-O bonding and shorter Ti-O distances between the topmost pair of planes and larger ones between this plane and the immediately lower plane (as the experimental results of Cabailh *et al.*[35] show). This pattern of displacements has a near perfect projection onto the eigenvectors of the soft mode of the bulk and the structure is therefore extremely compliant to this displacement pattern. Consequently the subsurface structure is distorted by a "frozen-in" phonon and the distortion propagates with decaying ampli-

tude to lower layers. This eigenvector displaces alternate layers in opposite directions. When in computational models with slab geometry and an odd number of layers, the displacements of the center layer are in phase and therefore doubled, leading to an increase in energy. In the case of an even number of layers, there is no center plane of atoms and the mismatch between the displacements propagating from the two surfaces is accommodated in the bonds, leading to a lower energy penalty.

V. CONCLUSIONS

The lattice dynamics of TiO_2 in the rutile structure displays a richness of behavior not fully revealed in earlier theoretical or experimental work. Our calculations sample the full Brillouin zone and reveal that in unstrained TiO_2 a TA mode is extremely soft (less than 50 cm^{-1}) over a substantial volume of reciprocal-space, a cigar-shaped region with axis along the line joining the halfway points of the **Γ**-**M** and **M**-**A** lines. Neither experiment nor the single previous calculation of phonon dispersion in rutile TiO_2 sampled this region, which explains why this mode has not been seen before. It is suggested that this soft mode could be studied using inelastic neutron or x-ray spectroscopy. The frequency is predicted to be significantly strain and through thermal expansion, temperature dependent. Therefore a temperature-dependent study should demonstrate significant softening and increased anharmonicity. We caution that this prediction is valid within the quasiharmonic approximation but may be modified within a full quantum treatment of the anharmonic nuclear motion. Such a treatment lies beyond the scope of the present work.

The low-frequency TA mode gives a non-negligible contribution to the vibrational free energy of the rutile phase and we conclude that careful *ab initio* thermodynamic studies of the relative phase stability of the rutile and anatase polymorphs must include a full sampling of the Brillouin zone. The common approximation of evaluating the vibrational free energy at only the **Γ** point gives a result in error by more than 25 meV, comparable to the difference in internal energy between the two phases.

The calculated behavior of the soft mode under strain gives additional possibilities for comparison with experiment. Like the **Γ** point A_{2u} ferroelectric mode, the frequency of the $(\frac{1}{2},\frac{1}{2},\frac{1}{4})$ TA mode decreases to zero under isotropic strain of 0.5–0.75 %. But because it is doubly degenerate and split by an anisotropic strain, the frequency decreases to zero under both expansive and compressional strains along [110]. While compression may be generated in conventional high-pressure cells, either expansion or compression may be generated by bending thin films grown on substrates.

We have also shown that in contrast to the behavior under a [001] strain, the A_{2u} ferroelectric mode does not become soft under an expansive [110] strain and indeed is quite insensitive to strain in this direction. Instead we predict that the Raman-active B_{2g} mode should soften under [110] uniaxial expansion and its frequency should decrease to zero at slightly over 1% strain. This softening may be observable experimentally using Raman spectroscopy. The strong crystal directionality dependence of these soft modes is perhaps not surprising but does demonstrate that well-oriented single-crystal samples will be required if such phenomena are to be observed experimentally.

Finally, the soft-mode behavior under uniaxial strain helps to explain some of the anomalous behavior discovered in several previous theoretical studies of the [110] surfaces of rutile TiO_2. Structural relaxation in the near-surface region is reasonably well approximated locally by a uniaxially strained bulk and it is precisely at this value of the bulk strain that the TA mode at $(\frac{1}{2},\frac{1}{2},\frac{1}{4})$ becomes soft. If we make the reasonable assumption that the elastic behavior of this region is modified in the same manner as of a similarly strained bulk crystal we predict that the surface lattice dynamics should also exhibit a soft mode. Such a soft mode could mediate long-ranged elastic interactions between surfaces in the slab geometry and cause the long-ranged oscillatory behavior with the number of layers in the model system reported in previous studies.

Recently, a paper appeared (Ref. 50), which also presents *ab initio* DFPT calculations for rutile TiO_2. LDA frequencies tabulated at the **Γ** point in that article agree with the last column of our Table II to 17 cm^{-1} or better. Dispersion curves are also presented which are in close agreement with our Fig. 1 in the segments common to both and confirm the features we discuss in Sec. III B. Those authors did not compute dispersion along the **M**-**A** line or anywhere where the anomalous softening is strong. Interestingly the dip halfway along **Γ**-**Z** which we attribute to the end point of the cigar-shaped low-frequency region is also visible in their Fig. 2.

ACKNOWLEDGMENTS

The authors would like to acknowledge the contribution of Amit Agarwal whose unpublished calculations (Ref. 31) first suggested the existence of the soft anomaly we describe. Computer time was provided by the Uppsala Multidisciplinary Center for Advanced Computational Science (UPPMAX) at Uppsala University and the Swedish National Infrastructure for Computing (SNIC) and by STFC's e-science facility SCARF.

[1] U. Diebold, Surf. Sci. Rep. **48**, 53 (2003).
[2] R. A. Parker, Phys. Rev. **124**, 1719 (1961).
[3] P. D. Mitev and K. Hermansson, Surf. Sci. **601**, 5359 (2007).
[4] C. Lee, P. Ghosez, and X. Gonze, Phys. Rev. B **50**, 13379 (1994).
[5] B. Montanari and N. M. Harrison, J. Phys.: Condens. Matter **16**, 273 (2004).
[6] B. Montanari and N. M. Harrison, Chem. Phys. Lett. **364**, 528

(2002).
[7] R. Sikora, J. Phys. Chem. Solids **66**, 1069 (2005).
[8] S. Baroni, S. de Gironcoli, A. Dal Corso, and P. Giannozzi, Rev. Mod. Phys. **73**, 515 (2001).
[9] M. Mikami, S. Nakamura, O. Kitao, and H. Arakawa, Phys. Rev. B **66**, 155213 (2002).
[10] S. J. Clark, M. D. Segall, C. J. Pickard, Ph. J. Hasnip, M. I. J. Probert, K. Refson, and M. C. Payne, Z. Kristallogr. **220**, 567 (2005).
[11] K. Refson, P. R. Tulip, and S. J. Clark, Phys. Rev. B **73**, 155114 (2006).
[12] J. P. Perdew and A. Zunger, Phys. Rev. B **23**, 5048 (1981).
[13] A. M. Rappe, K. M. Rabe, E. Kaxiras, and J. D. Joannopoulos, Phys. Rev. B **41**, 1227 (1990).
[14] N. A. W. Holzwarth, G. E. Matthews, R. B. Dunning, A. R. Tackett, and Y. Zeng, Phys. Rev. B **55**, 2005 (1997).
[15] J. S. Lin, A. Qteish, M. C. Payne, and V. Heine, Phys. Rev. B **47**, 4174 (1993).
[16] H. Monkhorst and J. Pack, Phys. Rev. B **13**, 5188 (1976).
[17] R. Restori, D. Schwarzenbach, and J. R. Schneider, Acta Crystallogr., Sect. B: Struct. Sci. **43**, 251 (1987).
[18] S. C. Abrahams and J. L. Bernstein, J. Chem. Phys. **55**, 3206 (1971).
[19] J. K. Burdett, T. Hughbanks, G. J. Miller, J. W. Richardson, and J. V. Smith, J. Am. Chem. Soc. **109**, 3639 (1987).
[20] G. Cangiani, Ph.D. thesis, Polytechnique Federale de Lausanne, 2003.
[21] F. Labat, P. Baranek, C. Domain, C. Minot, and C. Adamo, J. Chem. Phys. **126**, 154703 (2007).
[22] C. Lee and X. Gonze, Phys. Rev. B **49**, 14730 (1994).
[23] G. A. Samara and P. S. Peercy, Phys. Rev. B **7**, 1131 (1973).
[24] G. P. Francis and M. C. Payne, J. Phys.: Condens. Matter **2**, 4395 (1990).
[25] X. Gonze and C. Lee, Phys. Rev. B **55**, 10355 (1997).
[26] K. Parlinski, Z.-Q. Li, and Y. Kawazoe, Phys. Rev. Lett. **78**, 4063 (1997).
[27] N. J. Ramer and A. M. Rappe, Phys. Rev. B **59**, 12471 (1999).
[28] J. G. Traylor, H. G. Smith, R. M. Nicklow, and M. K. Wilkinson, Phys. Rev. B **3**, 3457 (1971).
[29] D. M. Eagles, J. Phys. Chem. Solids **25**, 1243 (1964).
[30] S. P. S. Porto, P. A. Fleury, and T. C. Damen, Phys. Rev. **154**, 522 (1967).
[31] A. Agarwal, M.Sc. thesis, King's College London, 2005.
[32] See supplementary material at http://link.aps.org/supplemental/10.1103/PhysRevB.81.134303 for additional table, figures, and movie.
[33] G. J. Ackland, M. C. Warren, and S. J. Clark, J. Phys.: Condens. Matter **9**, 7861 (1997).
[34] M. Hoesch (private communication).
[35] G. Cabailh, X. Torrelles, R. Lindsay, O. Bikondoa, I. Joumard, J. Zegenhagen, and G. Thornton, Phys. Rev. B **75**, 241403(R) (2007).
[36] E. A. Akhadov, S. A. Safron, J. G. Skofronick, D. H. Van Winkle, F. A. Flaherty, and R. Fatema, Phys. Rev. B **68**, 035409 (2003).
[37] T. Bredow, L. Giordano, F. Cinquini, and G. Pacchioni, Phys. Rev. B **70**, 035419 (2004).
[38] G. Li, J. Boerio-Goates, B. F. Woodfield, and L. Li, Appl. Phys. Lett. **85**, 2059 (2004).
[39] M. J. Harris, M. T. Dove, I. P. Swainson, and M. E. Hagen, J. Phys.: Condens. Matter **10**, L423 (1998).
[40] N. M. Harrison, X.-G. Wang, J. Muscat, M. Scheffler, and X. G. Wang, Faraday Discuss. **114**, 305 (1999).
[41] M. Ramamoorthy, D. Vanderbilt, and R. D. King-Smith, Phys. Rev. B **49**, 16721 (1994).
[42] A. Kiejna, T. Pabisiak, and S. W. Gao, J. Phys.: Condens. Matter **18**, 4207 (2006).
[43] S. J. Thompson and S. P. Lewis, Phys. Rev. B **73**, 073403 (2006).
[44] K. J. Hameeuw, G. Cantele, D. Ninno, F. Trani, and G. Iadonisi, J. Chem. Phys. **124**, 024708 (2006).
[45] H. Perron, C. Domain, J. Roques, R. Drot, E. Simoni, and H. Catalette, Theor. Chem. Acc. **117**, 565 (2007).
[46] P. Murugan, V. Kumar, and Y. Kawazoe, Phys. Rev. B **73**, 075401 (2006).
[47] P. J. D. Lindan, N. M. Harrison, M. J. Gillan, and J. A. White, Phys. Rev. B **55**, 15919 (1997).
[48] S. P. Bates, M. J. Gillan, and C. Kresse, Surf. Sci. **385**, 386 (1997).
[49] R. Lindsay, A. Wander, A. Ernst, B. Montanari, G. Thornton, and N. M. Harrison, Phys. Rev. Lett. **94**, 246102 (2005).
[50] E. Shojaee and M. R. Mohammadizadeh, J. Phys.: Condens. Matter **22**, 015401 (2010).